

Spatial Bandgap Engineering along Single Alloy Nanowires

Fuxing Gu,^{†,§} Zongyin Yang,^{†,§} Huakang Yu,[†] Jinyou Xu,[‡] Pan Wang,[†] Limin Tong,^{*,†} and Anlian Pan^{*,‡}

[†]State Key Laboratory of Modern Optical Instrumentation, Department of Optical Engineering, Zhejiang University, Hangzhou 310027, China

[‡]College of Physics and Microelectronics Science, Key Laboratory for Micro-Nano Physics and Technology of Hunan Province, Hunan University, Changsha 410082, China

S Supporting Information

ABSTRACT: Bandgap engineering of semiconductor nanowires is important in designing nanoscale multifunctional optoelectronic devices. Here, we report a facile thermal evaporation method, and realize the spatial bandgap engineering in single CdS_{1-x}Se_x alloy nanowires. Along the length of these achieved nanowires, the composition can be continuously tuned from $x = 0$ (CdS) at one end to $x = 1$ (CdSe) at the other end, resulting in the corresponding bandgap (light emission wavelength) being modulated gradually from 2.44 eV (507 nm, green light) to 1.74 eV (710 nm, red light). In spite of the existing composition (crystal lattice) transition along the length, these multicolor nanowires still possess high-quality crystallization. These bandgap engineered nanowires will have promising applications in such as multicolor display and lighting, high-efficiency solar cells, ultrabroadly spectral detectors, and biotechnology.

As the basic building blocks for next-generation nanoscale devices and integrated systems, semiconductor nanowires (NWs) have aroused increasing attention recently. Since bandgap is one of the most important parameters of semiconductor materials for optoelectronic applications, an important task in NW research is to achieve NWs with tunable band gaps. In the past years, several approaches have been developed to tune the NW composition and bandgap, such as hybrid pulsed laser ablation/chemical vapor deposition processes¹ and ion exchange reactions.² Also, based on the formation of alloys from two binary semiconductors, much work has been reported to show the capability of growing alloy NWs with continuously tunable composition or band gap,^{3–14} and even achieving spatial composition graded NWs on a single substrate.^{15–17} However, all the existing work involving the bandgap engineering of NWs is based on the composition tunability within narrow range or between different NWs, and wide-range bandgap engineering along a single NW has never been reported. In this work, we developed a source-moving thermal evaporation route and first realized the growth of a novel CdS_{1-x}Se_x alloy NW structures. Along the length of these achieved NWs, the composition can be continuously tuned from $x = 0$ (CdS) at one end to $x = 1$ (CdSe) at the other end of the same wire, thus, making these wires have a continuous light emission along their lengths from 507 nm (2.44 eV, green light) to 710 nm (1.74 eV, red light).

The source-moving growth approach was first investigated by Reimers et al. for the growth of composition-graded bulk CdSSe

alloy crystals in the 1960s.¹⁸ Here, we demonstrate a source-moving thermal evaporation route for composition-graded CdSSe NW growth in a horizontal quartz tube mounted inside a single-zone furnace. In the tube (inter diameter 45 mm, length 180 cm), an alumina boat (2 cm in width, 1 cm in height and 6 cm in length) with CdS powder (Alfa Aesar, 99.99% purity) was placed in the center of the heating zone, and another alumina boat with CdSe powder (Alfa Aesar, 99.995% purity) was placed upstream of the tube and outside the heating zone. The CdS and CdSe boats were separated by two empty alumina boats. A quartz push rod that was driven by a step motor through magnetic force was used to shift CdSe boats along the tube during the growth, as shown schematically in the experimental setup (see the Supporting Information Figure S1). Silicon wafers coated with a 2-nm thick gold film were placed downstream of the CdS powder to collect the deposited CdSSe NWs. A nitrogen gas flow was introduced into the system at a flow rate of 150 sccm to purge oxygen from the tube. After 20 min, the temperature in the center of the tube was elevated to 830 °C at a rate of 40 °C min⁻¹, while maintaining at 300 mba. After 40 min of growth, the CdSe powder was shifted downstream by the motor at a rate of 2.5 cm min⁻¹ until it reached the center of the heating zone, and at the same time the temperature was reduced at a rate of 0.5 °C min⁻¹ to 800 °C. After 1 h of growth at 800 °C, the temperature was reduced to room temperature.

A scanning electron microscopy (SEM) image shows that the synthesized CdSSe NWs have typical length up to 500 μm and diameter ranging from 100 to 1000 nm (see the Supporting Information Figure S2). Some wires are removed from the original as-grown sample and dispersed onto a MgF₂ substrate (refractive index ~1.39) for optical measurements.¹⁹ The real-color photograph of the dispersed wires under a 405-nm laser illumination shows that all the wires have multicolor photoluminescence (PL) emissions continuously varied from green to red along their lengths (Figure 1), indicating the gradual changing bandgap or composition along the length of the NWs. A certain portion of emissions was guided through and emitted out of these individual NWs at their ends, due to their high refractive indices and excellent structural uniformity for optical waveguiding,²⁰ as shown in the close-up SEM image of a single wire (see the Supporting Information Figure S3). The *in situ* Energy-dispersive spectrometry (EDS) along the total length of a typical wire shows that one end of the wire contains mainly elements Cd and S, while the other end of the wire is composed of elements Cd and Se (Figure S4).

Received: November 10, 2010

Published: January 27, 2011

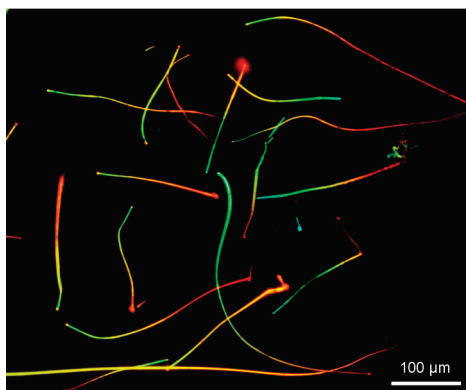


Figure 1. Real-color photograph of some CdSSe NWs dispersed on a low-index MgF₂ substrate under a 405-nm laser illumination.

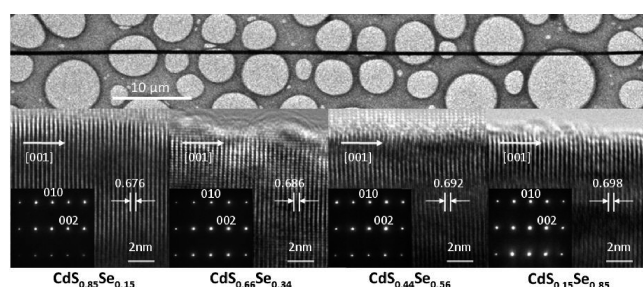


Figure 2. TEM image of a typical CdSSe NW (above) and its corresponding HRTEM images and SAED patterns taken from several representative regions along its length (below). The alloy compositions for each region are shown below the respective images.

The S concentration is complementary to that of Se along the length from the CdS end to the CdSe end, demonstrating that these as-grown wires are individually composition graded CdSSe nanostructures.

Transmission electron microscopy (TEM) was used to further investigate the structure of these composition graded CdSSe NWs. Figure 2 shows the TEM image of a typical wire (above) and its corresponding high-resolution TEM (HRTEM) images and selected-area electron diffraction (SAED) patterns taken from representative regions along its length (below). The alloy composition collected from the *in situ* TEM-EDS (see the Supporting Information Figure S5) is shown in the respective HRTEM images. The clear lattice profiles without apparent defects or phase segregations, as well as the well arrayed diffraction spots, indicate that the wire has high crystalline quality with hexagonal wurtzite structure. The wires were shown to grow along the [002] direction from the SAED results, while the (002) lattice spacing shows a continuous increase from the left to the right side along the length. This change in lattice spacing shows good agreement with the transition of S or Se concentration along the wires, verifying that the as-grown wires are composition graded CdSSe nanostructures.

Figure 3A gives the real-color photograph of a CdSSe NW illuminated using a beam of diffused 405-nm-wavelength laser, showing a very good color transition from green to red along its length. Panels B1–12 of Figure 3 show more clearly that different spots along the wire length have different PL color, and the color changes gradually from green to red when the wire was excited locally along the length with a beam of focused laser. The

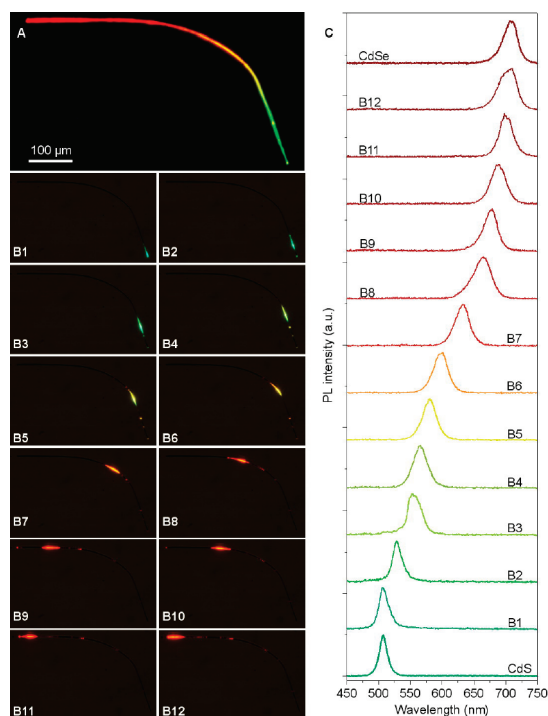


Figure 3. (A) Real-color photograph of a representative CdSSe NW illuminated under a beam of diffused 405-nm laser. (B1–12) Real-color photographs of different spots along the length, excited locally with a beam of focused 405-nm laser. (C) The corresponding local PL spectra collected from these excited spots in B1–12, respectively. The PL spectra of pure CdSe and CdS are also shown for comparison, respectively.

corresponding local PL spectra shown in Figure 3C (Curves B1–12) demonstrate that the PL spectra from every spot along the length have strong single-peak emission, with their peak wavelength continuously changed from 505 nm at one end to 710 nm at the other end of the wire. The peak wavelengths at both ends are consistent with those of pure CdS and CdSe, indicating that the as-grown wires have complete CdSSe composition tunability along their lengths.

Figure 4 gives the position-dependent compositions and bandgap values along the length of the multicolor CdSSe NW as shown in Figure 3. The bandgap values calculated from the EDS results (Figure S4) combined with the Vegard's law^{4a} (green rectangles) are in good agreement with those converted from the PL spectra (red circles), indicating that all the observed PL along the wires are from the band-edge emission that is tunable with the gradual changes of the local compositions along their lengths. The exhibited single band-edge emission, without any defect or structural disorder-related low-energy emission detected, further demonstrates that any spots along the entire length of the wires are highly crystallized alloys, with few defects or independent binary phases, which is consistent with the HRTEM observations.

As for the formation of these multicolor CdSSe NWs, the moving of the source materials during the growth plays a key role. The composition of the vapor–liquid–solid (VLS) induced NWs is determined by the available vapor concentration of the source materials. At the beginning of growth, the CdS powder at the central heating zone has a very high evaporation rate, while the CdSe powder, at a position upstream with a

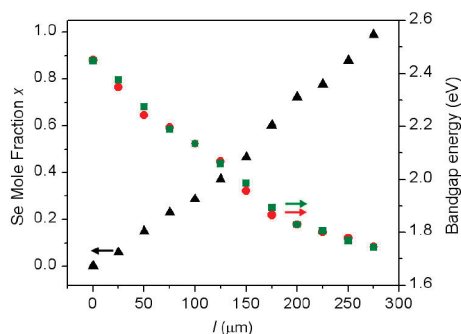


Figure 4. Position-dependent compositions and bandgap values along the length of the multicolor CdSSe NW. Se mole fraction values (black triangles) are obtained from the EDS results. Bandgap values are obtained from both the EDS compositions (green rectangles), and the PL spectra (red circles).

lower temperature, does not have any evaporation. Thus only CdS vapor is available and pure CdS NWs start to grow via the VLS process at the initial stage. As the growth proceeded, the CdS powder and the CdSe powder are pushed gradually by the step motor forward to the low temperature and the high temperature zone, respectively. Meanwhile, the CdS vapor concentration begins to decrease and the CdSe vapor concentration begins to increase. Thus, the composition of the newly grown wire material has a corresponding change with the change of respective vapor concentration, that is, S is gradually decreased and Se is gradually increased along the length of the wire. At last, the CdS powder is moved far away from the central heating zone to a low-temperature position where it has no more evaporation, while the CdSe powder reaches the central heating zone and has maximum evaporation. Thus, only pure CdSe vapor is available at the last stage of NW growth. From the side-view picture of the cross section of the as-grown sample under laser illumination, the color of emission changes from green at the root part of the wires, goes through yellow and orange, and finally turns into red at the top part of the wires (see the Supporting Information Figure S6), which gives a direct demonstration of the formation process discussed above. This source-moving growth route will be easily extended to the growth of multicolor alloy NWs of other material systems.

In summary, we have developed a source-moving thermal evaporation route and realized the growth of novel CdSSe alloy NW structures. Along the length of these achieved NWs, the composition can be continuously tuned from $x = 0$ (CdS) at one end to $x = 1$ (CdSe) at the other end of the same wire, thus, offering these wires a continuous light emission along their lengths from 507 nm (2.44 eV, green light) to 710 nm (1.74 eV, red light). These interesting nanostructures will have promising applications in multicolor display and lighting, high-efficiency solar cells, and ultrabroadly spectral detectors.

■ ASSOCIATED CONTENT

S Supporting Information. Schematical experimental setup for the multicolor NW growth; SEM image of the as-grown NWs; TEM-EDS spectra of several spots along the length of a representative wire; real-color photograph of an as-grown sample under laser illumination. This material is available free of charge via the Internet at <http://pubs.acs.org>.

■ AUTHOR INFORMATION

Corresponding Author

phytong@zju.edu.cn; Anlian.pan@gmail.com

Author Contributions

^SThese authors contributed equally.

■ ACKNOWLEDGMENT

This work was supported by the National Basic Research Programs of China (No. 2007CB307003), the National Natural Science Foundation of China (No. 60425517, 90923014 and 10974050), and the Aid program for Science and Technology Innovative Research Team in Higher Educational Institutions of Hunan Province.

■ REFERENCES

- (1) Wu, Y.; Fan, R.; Yang, P. *Nano Lett.* **2002**, *2*, 83.
- (2) (a) Jeong, U.; Xia, Y.; Yin, Y. *Chem. Phys. Lett.* **2005**, *416*, 246. (b) Li, G.; Jiang, Y.; Wang, Y.; Wang, C.; Sheng, Y.; Jie, J.; Zapien, J. A.; Zhang, W.; Lee, S.-T. *J. Phys. Chem. C* **2009**, *113*, 17183. (c) Zhang, B.; Jung, Y.; Chung, H.-S.; Vugt, L. V.; Agarwal, R. *Nano Lett.* **2010**, *10*, 149.
- (3) Qian, F.; Li, Y.; Gradedak, S.; Park, H.; Dong, Y.; Ding, Y.; Wang, Z. L.; Lieber, C. M. *Nat. Mater.* **2008**, *7*, 701.
- (4) (a) Pan, A. L.; Yang, H.; Liu, R.; Yu, R.; Zou, B.; Wang, Z. L. *J. Am. Chem. Soc.* **2005**, *127*, 15692. (b) Pan, A.; Wang, X.; He, P.; Zhang, Q.; Wan, Q.; Zacharias, M.; Zhu, X.; Zou, B. *Nano Lett.* **2007**, *7*, 2970. (c) Pan, A. L.; Liu, R.; Sun, M. H.; Ning, C. Z. *J. Am. Chem. Soc.* **2009**, *131*, 9502.
- (5) Persson, A. I.; Bjork, M. T.; Jeppesen, S.; Wagner, J. B.; Wallenberg, L. R.; Samuelson, L. *Nano Lett.* **2006**, *6*, 403.
- (6) Lorenz, M.; Kaidashev, E. M.; Rahm, A.; Nobis, T.; Lenzner, J.; Wagner, G.; Spemann, D.; Hochmuth, H.; Grundmann, M. *Appl. Phys. Lett.* **2005**, *86*, 143113.
- (7) Wang, M.; Fei, G. T.; Zhang, Y. G.; Kong, M. G.; Zhang, L. D. *Adv. Mater.* **2007**, *19*, 4491.
- (8) Liu, Y.; Zapien, J. A.; Shan, Y. Y.; Geng, C. Y.; Lee, C. S.; Lee, S. T. *Adv. Mater.* **2005**, *17*, 1372.
- (9) Hsu, H. C.; Wu, C. Y.; Cheng, H. M.; Hsieh, W. F. *Appl. Phys. Lett.* **2007**, *89*, 013101.
- (10) Kwon, S. J.; Choi, Y. J.; Park, J. H.; Hwang, I. S.; Park, J. G. *Phys. Rev. B* **2005**, *72*, 205312.
- (11) Shan, C. X.; Liu, Z.; Ng, C. M.; Hark, S. K. *Appl. Phys. Lett.* **2005**, *87*, 033108.
- (12) Venugopal, R.; Lin, P.; Chen, Y. T. *J. Phys. Chem. B* **2006**, *110*, 11691.
- (13) Liu, Y. K.; Zapien, J. A.; Shan, Y. Y.; Tang, H.; Lee, C. S.; Lee, S. T. *Nanotechnology* **2007**, *18*, 365606.
- (14) (a) Ouyang, L.; Maher, K. N.; Yu, C. L.; McCarty, J.; Park, H. *J. Am. Chem. Soc.* **2007**, *129*, 133. (b) Goebel, J. A.; Black, R. W.; Puthussery, J.; Giblin, J.; Kosel, T. H.; Kuno, M. *J. Am. Chem. Soc.* **2008**, *130*, 14822. (c) Agarwal, R. *Small* **2008**, *4*, 1872. (d) Tian, B.; Kempa, T. J.; Lieber, C. M. *Chem. Soc. Rev.* **2009**, *38*, 16.
- (15) Pan, A. L.; Zhou, W.; Leong, E. S. P.; Liu, R.; Chin, A. H.; Zou, B.; Ning, C. Z. *Nano Lett.* **2009**, *9*, 784.
- (16) Kyukendall, T.; Ulrich, P.; Aloni, S.; Yang, P. *Nat. Mater.* **2007**, *6*, 951.
- (17) Pan, A. L.; Liu, R.; Sun, M. H.; Ning, C. Z. *ACS Nano* **2010**, *4*, 671.
- (18) (a) Reimers, P.; Ruppel, W. *Phys. Status Solidi B* **1968**, *29*, K31. (b) Reimers, P. *Phys. Status Solidi B* **1969**, *35*, 707.
- (19) (a) Gu, F.; Zhang, L.; Yin, X.; Tong, L. *Nano Lett.* **2008**, *8*, 2757. (b) Gu, F.; Yu, H.; Wang, P.; Yang, Z.; Tong, L. *ACS Nano* **2010**, *4*, 5332.
- (20) Law, M.; Sirbully, D. J.; Johnson, J. C.; Goldberger, J.; Saykally, R. J.; Yang, P. D. *Science* **2004**, *305*, 1269.